CHARACTERIZATION AND THE SPECTRAL & PHOTOMETRIC BEHAVIOR OF MARS ANALOG COATED HAWAIIAN BASALT. S. A. Theuer*[1], M. S. Rice[1], M. D. Kraft[1], S. R. Mulcahy[1], K. Lapo[1], B. Garczynski[1], M. D. V. Gabbert[1], [1]Western Washington University (516 High St, Bellingham, WA 98225, USA, *theuers@wwu.edu)

Introduction: Visible to near-infrared (VNIR) reflectance spectroscopy is a commonly employed technique used to study the surface of Mars and other bodies, but spectra are sensitive to viewing geometry, nonlinear spectral mixing, and surface texture [e.g., 1,2]. The spectral influence of coatings and weathered materials atop basalt substrate on Mars is of particular interest, as coatings have been frequently identified and are known to impact VNIR spectral and photometric behavior [e.g., 3, 4]. Previous work using synthetic coatings and limited natural weathered materials has shown that coatings influence spectral slope, can impart unique photometric behavior, mask underlying lithologies, and may alter other absorption features [1,2,4], but further work is needed to characterize the formation mechanisms and spectral behavior of natural coatings, which display complex morphologies and compositions that impact spectra [5].

This work describes the composition, morphology, and the spectral and photometric behavior of natural coated Hawaiian basalt samples previously identified as reasonable analogs for potential coatings on Mars [e.g., 6,7]. The spectral characterization of these analog coatings provides valuable insight into the impact of coatings on VNIR spectra and will aid in our ability to interpret, identify, and distinguish coatings from unaltered lithologies using remotely sensed data from Mars and other bodies.

Methods: Basalt samples with varying amount of coating were collected from the 1920 Kilauea flow along the Kau Desert Trail (KD) and the 1970 Kilauea flow along the Puna Coast Trail (PC) in Hawaii Volcanoes National Park in August of 2022 and September of 2023. We qualitatively characterized coating composition and morphology using reflected light microscopy and Scanning Electron Microscope (SEM) with energy dispersive spectroscopy (EDS) elemental maps and backscattered electron (BSE) imaging. We collected small-diameter probe VNIR spectra from spot sizes of ~2 mm diameter to identify spectral end members [5]. Spectral and photometric behavior was characterized via hemispheric VNIR datasets collected using Western Washington University's spectrogoniometer, TANAGER [8] from surface areas of ~2.7 to 3.5 cm diameter at viewing geometries of -70 to +70 incidence and emission with 15-degree increments, and 0 to 135 azimuth with 45-degree increments.

Results: *Field Observations:* Coated areas of basalt on a scale of millimeters to 10s of meters were identified on pahoehoe, and less commonly a-a, flows in the field. In agreement with observations by [9], coatings were preferentially located on denser, pipe-bearing and breakout pahoehoe flows and less frequently on spongier, more vesicular flows prone to spalling. Localized areas of white fracture-infilling material were frequently observed in association with coated areas on all flow textures and field sites.

Microscopy & SEM: Three coating types were identified using microscopy, SEM, and EDS analysis (Figure 1 & 2): (1) a dusty blue, layered SiO_2 coating ("layered" coating); (2) a Fe/Ti-bearing coating that intermittently caps the layered coating and that correlates with the reddish and yellowish areas of coating ("Fe/Ti-bearing" coating); and (3) a white to transparent, porous SiO_2 coating containing fragments of mafic material that correlates with white surface and fracture-filling materials observed in the field ("porous" coating).

"Layered" SiO_2 coatings are more common than "porous" SiO_2 coatings, although we observed gradational transitions between the coating types. We found no uncoated surfaces (even seemingly uncoated dark surface areas exhibit thin, micron-scale SiO_2 rich coatings in SEM images). "Porous" coatings are predominantly composed of SiO_2, with some S, Fe, Al, Ti and other minor elements. "Porous" coatings do not follow the contours of the glassy basalt substrate surface as the "layered" coatings do, and instead overlay glassy basalt and "Fe/Ti-bearing" coatings intermittently along sample surfaces. "Layered" coatings are mostly SiO_2 and

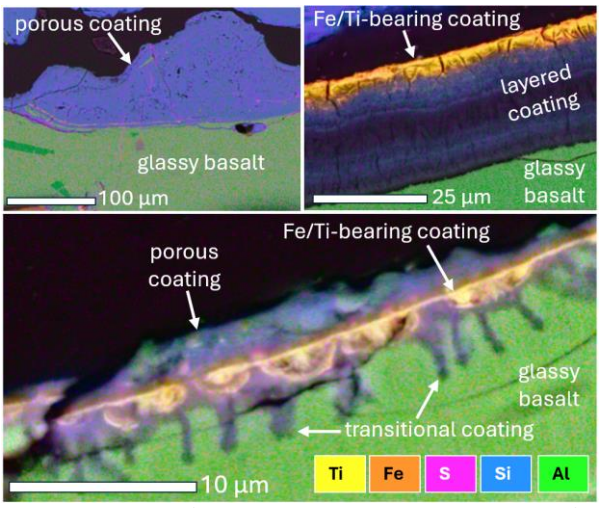

Figure 1: EDS maps of a coated PC sample showing the three identified coating types: "porous" SiO_2 rich coating and "layered" SiO_2 coating with a capping "Fe/Ti-bearing" layer of coating. A transitional zone shows "layered" coating forming beneath "porous" and "Fe/Ti-bearing" coating.

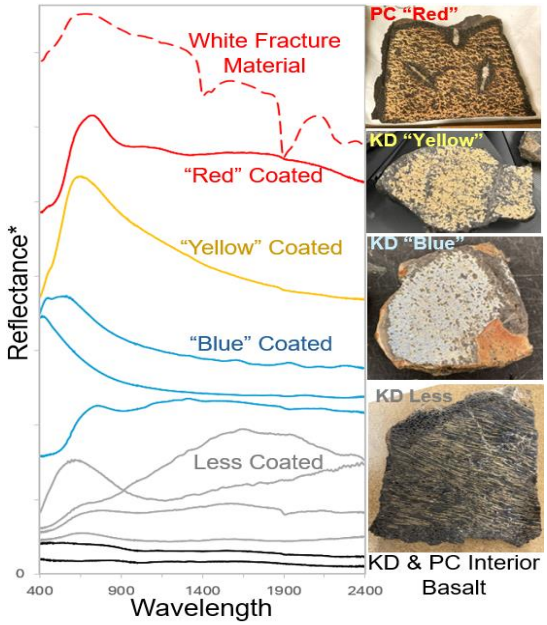

Figure 2: Small diameter probe VNIR spectral end members of sample surfaces, interior basalt spectra from a KD sample (top) and PC sample (bottom), and representative hand samples. White fracture material correlates with "porous" coating, red and yellow samples have significant "Fe/Ti-bearing" coating, blue samples have significant "layered" coating. *Spectra offset for clarity

are sometimes capped by a "Fe/Ti-bearing" layer [see 5,6,7]. Sulfur content varies across samples, but is commonly enriched in both "porous" and "layered" coating types (Figure 1).

VNIR Spectrogoniometry: Small-diameter probe spectra of "porous" white coatings display sharp absorption features at 1900 and 1410 nm, a feature at 2200 nm, a negative spectral slope in the NIR, and an overall spectral shape consistent with hydrated silica with some amount of iron oxides (Figure 2). The 1900, and 2200 nm absorption bands are present, though much shallower, in small-diameter probe spectra collected from surface areas of "layered" and "Fe/Ti-bearing" coating (Figure 2). The spectrum of interior basalt was notably masked by the spectral features of coatings, even when coatings were only present in small amounts on less coated samples (Figure 2).

In spectra at varying geometries, the NIR spectral slope (from 1400 nm to 2100 nm) for all samples is relatively negative in backscattering geometries and increasingly positive in forward scattering geometries, and increases with phase angle (e.g., Figure 3). This trend was most extreme for samples with significant amounts of Fe/Ti-bearing coatings, and was smaller in magnitude for less coated and spalled samples. Overall reflectance also generally increased with increasing phase angle. Spectral shape significantly smoothed and became less distinguishable with increasing phase angle. Absorption feature locations were not significantly

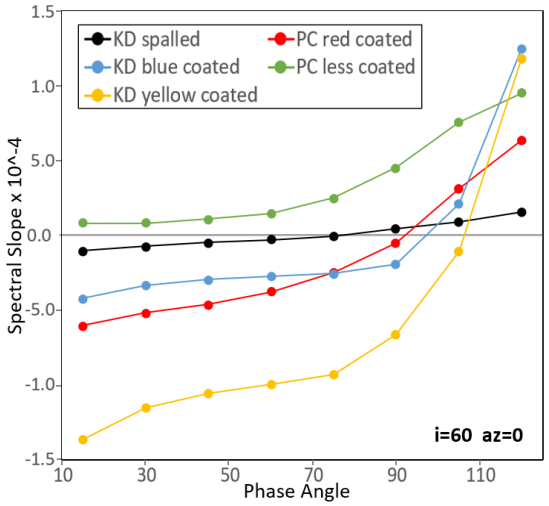

Figure 3: NIR spectral slope vs phase angle of representative samples calculated from 1400-2100 nm with i=60, az=0

altered with changing viewing geometry, though band depth for the ~1900 hydration feature, a weak but consistent feature in all spectra, decreased with increasing phase angle.

Discussion: Hawaiian analog coatings significantly mask underlying basalt spectral character and display notable photometric behavior, particularly related to NIR spectral slope and, to a lesser extent, band depth for hydration features. The increase in NIR spectral slope with increasing phase angle for coated samples, particularly for thickly coated samples, suggests that photometric analysis may assist in efforts to detect similar Si, Fe, and Ti-bearing coatings using remotely sensed spectral data.

Chemical analysis of coatings was largely consistent with observations by [5,6,7] in which two coating types were identified: a largely SiO_2 coating and a Fe/Ti-bearing layer, but an additional "porous" SiO_2 coating type was possible to identify on previous and new samples.

Further Work: More precise elemental compositions of coatings will be derived to better correlate coating composition with spectral character. Spectral data will be convolved to Mastcam-Z bandpasses [10,11] to aid in comparison to remotely sensed data from the surface of Mars and to better determine the impact of coatings within remotely sensed data.

Acknowledgments: Funding was provided by the NASA Solar System Workings Program and the NASA Mars-2020 Mission

References: [1] Rice M. S. et al. (2013) Icarus, 223, 499-533. [2] Curtis S. A. et al. (2022) LPSC, Abstract #2401. [3] Garczynski, B. J. et al. (2023) ESS, 056, 1670 [4] Fischer E. M. & Pieters C. M. (1993) Ica-rus, 102, 2, 185-202. [5] Theuer S.A. et al. (2023) LPSC, Abstract #1837. [6] Chemtob S. M. et al. (2010) JGR, 115, E04001. [7] Minitti M. E. et al. (2006) JGR, 112. [8] Rice M. S. et al. (2022) LPSC, Abstract #2570. [9] Chemtob S. M. et al. (2014) JVGR, 286, 41-54. [10] Rice M. S. et al. (2023) JGR, 128. [11] Bell J. F. et al. (2021) Space Sci Rev, 217, 24